TECHNICAL ARTICLE

X-ray powder reference patterns of the Fe($Sb_{2+x}Te_{1-x}$) skutterudites for thermoelectric applications

W. Wong-Ng,[1,a] J.A. Kaduk,[2] G. Tan,[3] Y. Yan,[3] and X. Tang[3]
[1]*Materials Science Measurement Division, National Institute of Standards and Technology, Gaithersburg, Maryland 20899*
[2]*Department of Biological and Chemical Sciences, Illinois Institute of Technology, Chicago, Illinois 60616*
[3]*State Key Laboratory of Advanced Technology for Materials Synthesis and Processing, Wuhan University of Technology, Wuhan, Hubei 430070, China*

(Received 16 December 2013; accepted 20 March 2014)

The crystal structure and powder X-ray diffraction (XRD) patterns for three skutterudite samples, Fe($Sb_{2+x}Te_{1-x}$), $x = 0.05$, 0.10, 0.20, have been determined. These compounds crystallize in the cubic space group $Im\bar{3}$. Te was found to randomly substitute in the Sb site. Because of the fact the covalent radius of Sb is greater than that of Te, a trend of increasing lattice parameter has been observed as the x value in Fe($Sb_{2+x}Te_{1-x}$) increases [cell parameters range from 9.10432(4) to 9.11120(3) Å for $x = 0.0$ to 0.2, respectively]. The Fe–Sb/Te bond distance also increases progressively [from 2.5358(4) to 2.5388(4) Å] as the Te content decreases. While average Sb/Te–Sb/Te distances in the four-membered rings are similar in these three compounds, the average Sb/Te–Sb/Te edge distances in the octahedral framework increase progressively from 3.5845(12) to 3.5900(13) Å. Reference XRD patterns of these three phases have been prepared to be included in the Powder Diffraction File (PDF). © *2014 International Centre for Diffraction Data.* [doi:10.1017/S0885715614000347]

Key words: thermoelectric materials, Fe($Sb_{2+x}Te_{1-x}$) skutterudites, X-ray powder reference patterns, crystal structure.

I. INTRODUCTION

Energy conversion research is important in recent years for the potential improvement of efficiency of energy utilization. Thermoelectric (TE) materials are known for their ability for either cooling or waste heat conversion applications. The performance of TE materials is judged by the dimensionless figure-of-merit (ZT) of the material, given by $ZT = S^2\sigma T/\kappa$, where T is the absolute temperature, S is the Seebeck coefficient or TE power, σ is the electrical conductivity, and k is the thermal conductivity (Nolas *et al.*, 2001).

Among a number of potential classes of TE materials that are widely studied (clathrates, half-Heusler, skutterudites, cobaltates, etc.); skutterudite compounds with general structure type of $CoSb_3$ exhibit high potential for TE applications. Extensive efforts have been conducted concerning the property improvement of skutterudite materials either via substitution or via nano-composite formation (Fleurial *et al.*, 1997a, b; Liu *et al.*, 2008; Yang *et al.*, 2011; Su *et al.*, 2012). For example, one way to lower the thermal conductivity of a binary skutterudite is the formation of a ternary phase by isoelectronic substitution. This substitution can be either performed at the anionic site by a pair of elements from 14th to 16th groups [e.g., $CoSn_{1.5}Se_{1.5}$ (Laufek *et al.*, 2009), $InGe_{1.5}Se_{1.5}$ (Laufek and Navrátil, 2010), and $InGe_{1.5}Se_{1.5}$ (Vaqueiro *et al.*, 2006)], or by isoelectronic substitution at the cationic site by a pair of elements from 8th to 10th groups [e.g., $Fe_{0.5}Ni_{0.5}Sb_3$ (Navrátil *et al.*, 2012)].

Tan *et al.* (2013) reported high TE figures of merit (ZT) for the $FeSb_{2+x}Te_{1-x}$ materials (ternary skutterudite series that are derived from $CoSb_3$), with the largest ZT value reaching ~0.65 for the sample with $x = 0.2$. This is the highest value among all p-type unfilled skutterudites and is comparable with filled n-type compositions such as Te-doped $CoSb_3$ with ZT about 0.7 (Li *et al.*, 2005). Figure 1 gives the ZT plot vs. x for $FeSb_{2+x}Te_{1-x}$ ($x = 0$, 0.05, and 0.1) (Tan *et al.*, 2013). $FeSb_2Te$ shows anomalous electrical and thermal transport properties. Considerable modification in band structure induced by Fe and mixed (Fe^{2+} and Fe^{3+}) valence states scattering of phonons was described (Tan *et al.*, 2013). Substitution of Te by Sb results in increasing the hole concentration without significantly affecting the band structure. As a result of the enhanced density of states, substantial improvement of electrical conductivity while maintaining high Seebeck coefficient was achieved. Furthermore, the heat carrying phonons are strongly scattered with the increasing value of x in $FeSb_{2+x}Te_{1-x}$ because of the formation of solid solutions between two end members: □$FeSb_2Te$ and □$FeSb_3$ (where □ can be viewed as a vacancy).

This paper has two main goals. The first is to report the crystallography and crystal chemistry for three members of the $FeSb_{2+x}Te_{1-x}$ ($x = 0.05$, 0.10, 0.20) series. Since X-ray diffraction (XRD) patterns are critical for phase characterization, the second goal of this study is to provide the experimental X-ray powder diffraction patterns for these $FeSb_{2+x}Te_{1-x}$ phases for supplementing the Powder Diffraction File, (2014).

[a]Author to whom correspondence should be addressed. Electronic mail: winnie.wong-ng@nist.gov

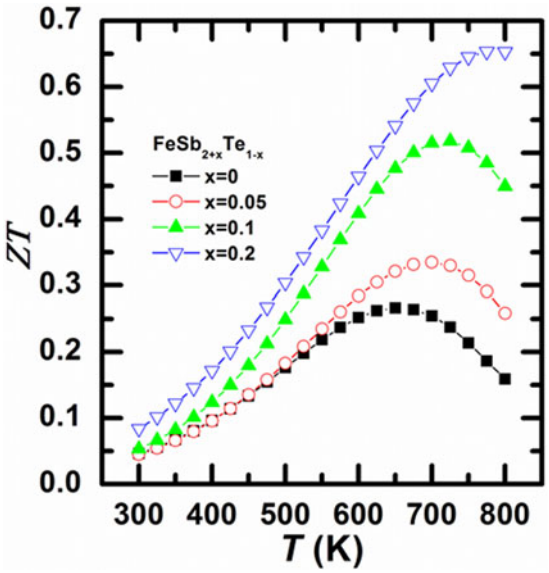

Figure 1. (Color online) Plot of ZT values of $FeSb_{2+x}Te_{1-x}$ ($x = 0$, 0.05, 0.1, and 0.2) as a function of temperature (Tan *et al.*, 2013).

II. EXPERIMENTAL

A. Sample preparation

High-purity Fe (99.5%, shot), Sb (99.9999%, shot), and Te (99.99%, shot) were weighed according to the $FeSb_{2+x}Te_{1-x}$ ($x = 0.05$, 0.1, 0.2) stoichiometry and sealed in silica tubes under10^{-3} Pa pressure. After the charge was melted and homogenized at 1373 K for 12 h, the ampoules were quenched in a supersaturated saltwater bath and subsequently annealed at 853 K for 7 days. The resulting ingots were ground into fine powders and then sintered by spark plasma sintering (SPS) at 803 K for 5 min under the pressure of 40 MPa.

B. Powder XRD and reference pattern preparation[1]

The samples were deposited as acetone slurries on a quartz zero-background cell. X-ray powder patterns were measured on a Bruker D2 Phaser diffractometer (30 kV, 10 mA, 5°–130° 2θ in 0.0202144° steps, 1 s step^{-1}) equipped with a LynxEye position-sensitive detector.

The Rietveld refinement technique (Rietveld, 1969) with the software suite GSAS (Larson and von Dreele, 2004) was used to refine the structures of $FeSb_{2+x}Te_{1-x}$. A structure model of $CoSb_3$ reported previously (Oftedal, 1928) was used for the initial model. The GSAS profile function #4 was used with refinement on the specimen displacement and the size broadening term, LX. The reported peak positions were calculated from the lattice parameters. When peaks are not resolved at the resolution function, the intensities are summed, and an intensity-weighted d-spacing is reported. They are also corrected for systematic errors both in d-spacing and intensity.

[1] Certain trade names and company products are mentioned in the text or identified in illustrations in order to adequately specify the experimental procedures and equipment used. In no case does such identification imply recommendation or endorsement by the National Institute of Standards and Technology.

TABLE I. Rietveld refinement results for $Fe(Sb_{2+x}Te_{1-x})$.

X	0.05	0.1	0.2
WR_p	0.0504	0.0528	0.0538
R_p	0.0388	0.0358	0.0402
χ^2	1.622	3.109	1.804
#Obs refl	5837	5837	5837
#Variables	17	17	17
$R(F)$	0.0698	0.0647	0.0815
$R(F^2)$	0.0633	0.0755	0.0782

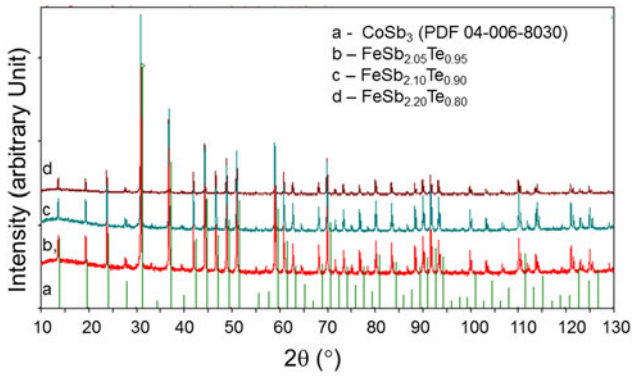

Figure 2. (Color online) Powder XRD patterns of $FeSb_{2+x}Te_{1-x}$ with $x =$ 0.05, 0.10, and 0.20, and stick pattern of $CoSb_3$ from the ICDD database (04-006-8030).

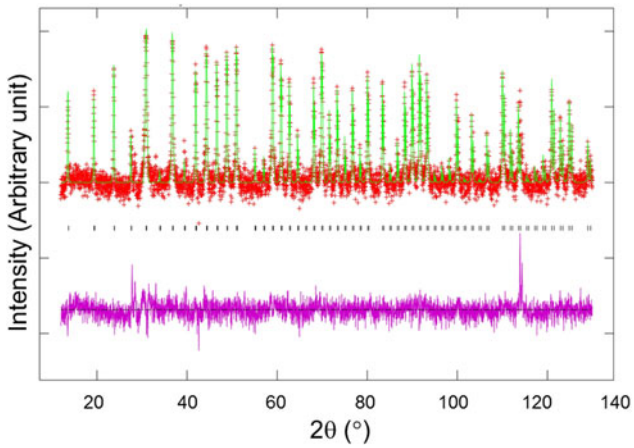

Figure 3. (Color online) Observed (crosses), calculated (solid line), and difference XRD pattern (bottom) for $FeSb_{2.2}Te_{0.8}$ by the Rietveld analysis technique. The difference pattern is plotted at the same scale as the other calculated peak positions. The peak at ≈113.9° 2θ is from an inclusion in the zero-background quartz holder.

III. RESULTS AND DISCUSSION

The Rietveld refinement results of the three skutterudite samples, $FeSb_{2+x}Te_{1-x}$ with $x = 0.05$, 0.10, and 0.20, are shown in Table I. The powder XRD patterns of these compounds compare well with the stick pattern of $CoSb_3$ from the ICDD database (88–2437) (Figure 2). Figure 3 is a Rietveld plot for $FeSb_{2.2}Te_{0.8}$ as an example. The observed (crosses), calculated (solid line), and difference XRD patterns (bottom) for $FeSb_{2.2}Te_{0.8}$ are shown. No impurity phase was found in these three samples.

https://doi.org/10.1017/S0885715614000347 Published online by Cambridge University Press

TABLE II. Lattice parameters, unit-cell volumes and calculated densities for $Fe(Sb_{2+x}Te_{1-x})$ (space group $Im\bar{3}$).

x	a (Å)	V (Å^3)	Dx (g cm^{-3})
0.05	9.10515(3)	754.81	7.51
0.10	9.10688(3)	755.23	7.50
0.20	9.11120(3)	756.32	7.48

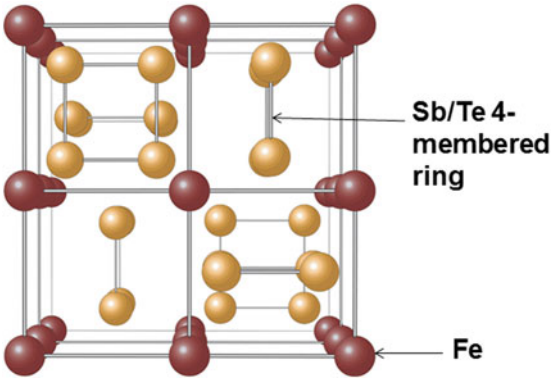

Figure 4. (Color online) View of the $FeSb_{2+x}Te_{1-x}$ structure (cubic, $Im\bar{3}$) along the a-axis showing Fe atoms and the rectangular Sb/Te rings (Prytz, 2007).

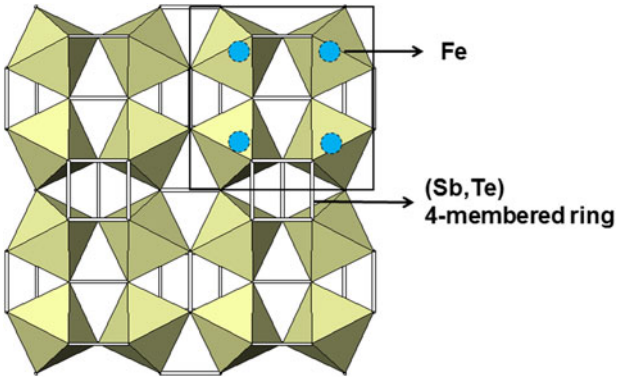

Figure 5. (Color online) Crystal structure of skutterudites $FeSb_{2+x}Te_{1-x}$ featuring distorted Sb/Te octahedral (Cubic, $Im\bar{3}$) and four-membered Sb/Te rings.

Table II gives the lattice parameters for $FeSb_{2+x}Te_{1-x}$. As the covalent radius of Sb (1.40 Å) is greater than that of Te (1.36 Å) (Pyykko and Atsumi, 2009), the calculated density values, D_x, decreases as the value of x increases.

The skutterudite compounds, $FeSb_{2+x}Te_{1-x}$, crystallize in the cubic space group $Im\bar{3}$ (No. 204) (Oftedal, 1928). The unit cell of this structure can also be viewed as built from eight smaller cubes with the Fe atoms residing in the cube vertices. Six of these cubes are filled with nearly square planar rings formed by the Sb/Te atoms; these rings are oriented almost parallel to one of the unit-cell edges (Figure 4) (Sales, 2003; Prytz, 2007). The structure of $FeSb_{2+x}Te_{1-x}$ can also be described as a corner-sharing octahedral network, where the icosahedral voids at 2a position of the $Im\bar{3}$ space group are empty. The Fe atoms are located in the centers of the trigonally distorted octahedral voids with Sb/Te residing in the void apexes (Figure 5). The unit-cell of $FeSb_{2+x}Te_{1-x}$ (ranging from 754.81 to 756.32 Å^3) are in general smaller than the volumes of skutterudites, which have the icosahedral voids filled by Ca, Ce or Ca/Ce atoms [$CeFe_4Sb_{12}$ (763.49 Å^3), $CaFe_4Sb_{12}$ (769.80 Å^3), and $(Ca_{0.5}Ce_{0.5})Fe_4Sb_{12}$ (765.82 Å^3)] (Yan *et al.*, 2014).

In the refined structural model of $FeSb_{2+x}Te_{1-x}$, the only free atomic coordinates are those of the Sb/Te atoms, which occupy the position is 24 g with 0yz coordinates. The planar rings formed by Sb/Te acquire an ideal square shape only if $y + z = ½$ (Oftedal, 1928; Kjekshus *et al.*, 1973,1974) is fulfilled. Perfect octahedral coordination for the Fe atoms requires condition $y(2z - 1) = z - 3/8$, and an ideal icosahedral environment around 2a position requires $y^2 = z^2 + yz$. Therefore, deviation from the above relations (Table III) yields rectangular rings instead of square shape, a trigonally distorted octahedron, and distorted icosahedral symmetry for the Sb/Te atoms. For example, the ratio between the short and long distance in these rectangular rings are all 0.94 for $x = 0.05$, 0.1, and 0.2 in the $FeSb_{2+x}Te_{1-x}$ samples as compare to the ratio of 0.97 in the $CoSb_3$ compound (Kjekshus *et al.*, 1974).

The refined bond distances are reported in Table IV. A trend was observed in the Fe–Sb/Te distances, that is, as x increases in $FeSb_{2+x}Te_{1-x}$, the Fe–Sb/Te distance increases [from 2.5358(4) to 2.5388(4) Å]. The average Sb/Te–Sb/Te distances in the four-rectangular rings are similar in these three compounds [≈2.973(2) Å average]. This average distance is slightly longer than that found in $RuSb_2Te$ [average of 2.952(3) Å] (Laufek and Navrátil, 2011), and is significantly longer than the ideal Sb–Sb distance of 2.80 Å (Pyykko and Atsumi, 2009). The average Sb/Te–Sb/Te edge distances in the octahedral framework, on the other hand, increase progressively from 3.5845(12) to 3.5900(13) Å as "x" increases.

Powder diffraction patterns of three different skutterudites, with $x = 0.05$, 0.10, and 0.20, have been prepared and

TABLE III. Refined structural parameters for $Fe(Sb_{2+x}Te_{1-x})$ (space group $Im\bar{3}$). The position 2a (0,0,0) is vacant in all samples.

Atoms	x	y	z	U(Å^2)	Frac	Wycoff position
(i) $x = 0.05$						
Fe	¼	¼	¼	0.0126(8)	1.0	8c
Sb/Te	0	0.1581(1)	0.3314(1)	0.0150(2)	0.683/0.317	24g
(ii) $x = 0.10$						
Fe	¼	¼	¼	0.0093(2)	1.0	8c
Sb/Te	0	0.1578(1)	0.3314(1)	0.0150(2)	0.700/0.300	24g
(iii) $x = 0.20$						
Fe	¼	¼	¼	0.0122(8)	1.0	8c
Sb/Te	0	0.1579(1)	0.3316(1)	0.0146(2)	0.733/0.267	24g

https://doi.org/10.1017/S0885715614000347 Published online by Cambridge University Press

TABLE IV. Interatomic distances, d (Å), in $Fe(Sb_{2+x}Te_{1-x})$, M = Sb/Te

Atom–atom	0.05	0.1	0.2
Fe–M × 6	2.5358(4)	2.5375(4)	2.5388(4)
Rectangular ring (Figure 3):			
M–M × 2	2.879 (2)	2.874(2)	2.877(2)
M–M × 2	3.071(2)	3.070(2)	3.069(2)
Ave. M–M	2.975(2)	2.972(2)	2.973(2)
Ratio of short/long distance	0.937	0.936	0.937
Octahedral edges (Figure 4):			
M–M × 4	3.4725(10)	3.4754(11)	3.4758(10)
M–M × 4	3.6965(15)	3.7020(15)	3.7042(15)
Ave. M–M	3.5845(12)	3.5887(13)	3.5900(13)

TABLE V. X-ray powder pattern, $FeSb_{2+x}Te_{1-x}$ ($x = 0.2$) ($Im\bar{3}$), $a = 9.11120(3)$ Å, $V = 756.32(6)$ Å^3, $D_x = 7.48$ g cm^{-3}. The "d" values are calculated from the lattice parameters. The symbols "M" and " + " refer to peaks containing contributions from two and more than two reflections, respectively. The symbol * indicates the particular peak has the strongest intensity of the entire pattern and is designated a value of "999".

d	I	h	K	l	d	I	h	k	l	d	I	h	k	l
6.4426	51	1	1	0	4.5556	50	2	0	0	3.7196	84	2	1	1
3.2213	15	2	2	0	2.8812	999	3	0	1M	2.4351	999	3	1	2M
2.2778	8	4	0	0	2.1475	95	3	3	0M	2.0373	254	4	0	2M
1.9425	100	3	3	2	1.8598	174	4	2	2	1.7869	224	4	1	3 +
1.6635	3	5	2	1 +	1.6107	4	4	4	0	1.5626	266	5	0	3 +
1.5185	110	4	4	2M	1.4780	59	5	3	2	1.4406	10	6	2	0M
1.3736	55	6	2	2	1.3434	192	6	1	3M	1.3151	23	4	4	4
1.2885	44	5	3	4	1.2635	10	6	0	4M	1.2399	44	6	3	3 +
1.2175	7	6	2	4	1.1964	71	7	3	0M	1.1571	64	7	3	2 +
1.1215	7	8	1	1	1.1049	58	6	4	4 +	1.0890	91	6	5	3M
1.0738	110	8	2	2M	1.0187	4	8	4	0	1.0062	41	9	1	0 +
0.9825	23	9	2	1	0.9604	16	9	3	0 +	0.9398	101	7	6	3 +
0.9299	20	8	4	4	0.9204	52	9	4	1 +	0.8850	71	9	4	3 +
0.8767	33	6	6	6	0.8687	60	10	1	3 +	0.8533	17	8	1	7 +

submitted to the PDF. An example of the reference pattern of $FeSb_{2+x}Te_{1-x}$ ($x = 0.2$) is given in Table V. The intensity values reported are integrated intensities rather than peak heights. All patterns have been submitted for inclusion in the Powder Diffraction File, (2014).

IV. SUMMARY

X-ray powder diffraction patterns of single-phase $FeSb_{2+x}Te_{1-x}$ ($x = 0.05$, 0.1, 0.2), which have excellent TE properties have been prepared and submitted to ICDD for inclusion in the PDF. These skutterudite materials crystallize in the cubic system with space group $Im\bar{3}$, and their cell parameters range from 9.10432(4) to 9.11120(3) Å (for x = 0.0 to 0.2, respectively). The unit-cell volume of $FeSb_{2+x}Te_{1-x}$ (ranging from 754.81 to 756.32 Å^3) is in general smaller than those cells that have atoms filled in the distorted icosahedral voids. As the x increases in $FeSb_{2+x}Te_{1-x}$, the Fe–Sb/Te distance increases [from 2.5358(4) to 2.5388(4) Å].

ACKNOWLEDGEMENTS

This work was partially supported by the International Centre for Diffraction Data (Grants-in-aid project), National Basic Research Program of China (Grant No. 2013CB632502), the Natural Science Foundation of China (Grant Nos. 51172174 and 51002112), and International Science & Technology Cooperation Program of China (Grant No. 2011DFB60150) along with 111 Project (Grant No. B07040).

Fleurial, J. P., Caillat, T., and Borshchevsky, A. (**1997a**). Skutterudites: an update, in Proceedings of the 16th International Conference on Thermoelectrics, (IEEE, Piscataway, NJ) p. 1–11.

Fleurial, J. P., Caillat, T., and Borshchevsky, A. (**1997b**). "Low thermal conductivity skutterudites," MRS Proc. **478**, 175. doi: 10.1557/PROC-478-175.

Kjekshus, A., Nicholson, D. G., and Rakke, T. (**1973**). "Compounds with the skutterudite type crystal structure. I. On Oftedal's relation," Acta Chem. Scand. **27**, 1307–1314.

Kjekshus, A., Nicholson, D. G., and Rakke, T. (**1974**). "Compounds with the skutterudite type crystal structure. III. structural data for arsenides and antimonides," Acta Chem. Scand. **A28**, 99–103.

Larson, A. C. and von Dreele, R. B. (**2004**). *General Structure Analysis System (GSAS)*, Los Alamos National Laboratory Report LAUR 86–748, Los Alamos, USA: Los Alamos National Laboratory.

Laufek, F. and Navrátil, J. (**2010**). "Crystallographic study of ternary ordered skutterudite $IrGe_{1.5}Se_{1.5}$," Powder Diffr. **25**, 247–252.

Laufek, F. and Navrátil, J. (**2011**). "Synthesis and Rietveld refinement of the ternary skutterudite $RuSb_2Te$," Powder Diffr. **26**, 331–334.

Laufek, F., Navrátil, J., Plašil, J., Plechĉcek, T., and Draŝar, Ĉ. (**2009**). "Synthesis, crystal structure and transport properties of skutterudite-related $CoSn_{1.5}Se_{1.5}$," J. Alloys Compd. **479**, 102–106.

Li, X. Y., Chen, L. D., Fan, J. F., Zhang, W. B., Kawahara, T., and Hirai, J. (**2005**). "Thermoelectric properties of Te-doped $CoSb_3$ by spark plasma sintering," Appl. Phys. **98**, 083702.

Liu, W. S., Zhang, B. P., Zhao, L. D., and Li, J. F. (**2008**). "Improvement of thermoelectric performance of $CoSb_{3-x}Te_x$ skutterudite compounds by

additional substitution of IVB-group elements for Sb," Chem. Mater., **20**, 7526–7531.

Navrátil, J., Laufek, F., Plcháček, T., and Drašar, Č. (**2012**). "Thermoelectric properties of the $Ru_2Ni_2Sb_{12}$ ternary skutterudite," J. Solid State Chem., **193**, 2–7.

Nolas, G. S., Sharp, J., and Goldsmid, H. J. (**2001**). *Thermoelectric: Basic Principles and New Materials Developments* (Springer, New York).

Oftedal, I. (**1928**). "The crystal structure of skutterudite and smaltite-chloanthite," Z. Kristallogr. **A66**, 517.

Powder Diffraction File (**2014**). Produced by International Centre for Diffraction Data, 12 Campus Blvd., Newtown Squares, PA. 19073-3273, USA.

Prytz, Ø. (**2007**). "Electronic structure and bonding in thermoelectric skutterudites," PhD thesis, Physics Department, University of Oslo.

Pyykko, P. and Atsumi, M. (**2009**). "Molecular single-bond covalent radii for elements 1–118," Chem. Eur. J. **15** (1), 186.

Rietveld, H. M. (**1969**) "A profile refinement method for nuclear and magnetic structures," J. Appl. Crystallogr. **2**, 65–71.

Sales, B. C. (**2003**). *Handbook on the Physics and Chemistry of Rare-Earths* (Elsevier Science, Amsterdam), Vol. **33**, p. 1.

Su, X., Li, H., Yan, Y., Wang, G., Chi, H., Zhou, X., Tang, X., Zhang, Q., and Uher, C. (**2012**). "Microstructure and thermoelectric properties of $CoSb_{2.75}Ge_{0.25-x}Te_x$ prepared by rapid solidification," Acta Mater. **60**, 3536–3544.

Tan, G., Liu, W., Chi, H., Su, X., Wang, S., Yan, Y., Tang, X., Wong-Ng, W., and Uher, C. (**2013**). "Realization of high thermoelectric performance in p-type unfilled ternary skutterudites $FeSb_{2+x}Te_{1-x}$ via band structure modification and significant point defect scattering," Acta Mater., **61**, 7693–7704.

Vaqueiro, P., Sobany, G. G., Powell, A. V., and Knight, K. S. (**2006**). "Structure and thermoelectric properties of the ordered skutterudite CoGe1.5Te1.5," J. Solid State Chem. **179**, 2047–2053.

Yan, Y. G., Wong-Ng, W., Li, L., Levin, I., Kaduk, J. A., Suchomel, M. R., Sun, X., Tan, G. J., and Tang, X. F. (**2014**). "Structures and thermoelectric properties of double-filled $(Ca_xCe_{1-x})Fe_4Sb_{12}$ skutterudites," J. Appl. Phys. (2014, submitted).

Yang, J., Qiu, P., Liu, R., Xi, L., Zheng, S., Zhang, W., Chen, L., Singh, D. J., Yang, J. (**2011**). "Trends in electrical transport of *p*-type skutterudites RFe_4Sb_{12} (R = Na, K, Ca, Sr, Ba, La, Ce, Pr, Yb) from first-principles calculations and Boltzmann transport theory," Phys. Rev. B **84**, 235205.

https://doi.org/10.1017/S0885715614000347 Published online by Cambridge University Press